

# Direct Analysis of Sedimentation Equilibrium Distributions Reflecting Complex Formation between Dissimilar Reactants<sup>†</sup>

Donald J. Winzor,<sup>\*,‡</sup> Michael P. Jacobsen,<sup>‡,§</sup> and Peter R. Wills<sup>||</sup>

Center for Protein Structure, Function and Engineering, Department of Biochemistry, University of Queensland, Brisbane, Queensland 4072, Australia, Department of Physics, University of Auckland, Auckland, New Zealand, and Santa Fe Institute, 1399 Hyde Park Road, Santa Fe, New Mexico 87501

Received September 8, 1997; Revised Manuscript Received December 11, 1997

**ABSTRACT:** Procedures are developed for the characterization of thermodynamically ideal complex formation between dissimilar macromolecular reactants by direct analysis of sedimentation equilibrium distributions. Studies of an electrostatic interaction between ovalbumin and cytochrome *c* are used to illustrate the application of analyses pertaining to (i) the situation in which separate sedimentation equilibrium distributions for the two macromolecular constituents are available, (ii) that in which the experimental record reflects the distribution of only one constituent, and (iii) the situation in which a composite distribution for both constituents is the sole experimental record. An association constant of 63 000 ( $\pm$  2000) M<sup>-1</sup> is obtained for the 1:1 interaction between ovalbumin and cytochrome *c* under the conditions examined (pH 6.3, *I* 0.03). Because of their inherent simplicity, these direct analytical procedures offer potential for accommodating the effects of thermodynamic nonideality in dissimilar reactant systems.

Despite the greater biological prevalence of interactions between dissimilar macromolecular reactants, protein self-association has been the predominant phenomenon studied by sedimentation equilibrium. However, the introduction of a new generation of analytical ultracentrifuges has kindled interest in the use of this technique for the characterization of heterogeneous associations (1–4). A common feature of these studies has been their evaluation of the binding constant by iterative simulation of sedimentation equilibrium distributions to obtain the best-fit description of the experimental distributions for the two solute constituents—a protocol analogous to that frequently used for the characterization of solute self-association (5). For many years a problem with such analyses has been their inability to accommodate realistically the effects of thermodynamic nonideality in either self-associating or heterogeneously associating systems—a problem eliminated recently for the former by the development of a noniterative method of allowance for the effects of thermodynamic nonideality on the statistical–mechanical basis of excluded volume (6). Encouraged by the successful development of that direct analysis of self-association incorporating rigorous statistical–mechanical treatment of thermodynamic nonideality (6), we now turn attention to the feasibility of employing a similar approach for the study of interactions between dissimilar solutes.

As in that previous study of solute self-association, the starting point for the direct analysis of heterogeneous association has been the  $\Omega$  function (7–9), the attraction of which is its ability to provide information on the thermodynamic activity of the smallest solute species throughout a sedimentation equilibrium distribution. However, advantage is again taken of the fact that a slight adaptation of the  $\Omega$  treatment allows this feature to be exploited to even greater effect (6). Results obtained with mixtures of cytochrome *c* and ovalbumin are used to illustrate the application of quantitative expressions developed for the evaluation of association equilibrium constants by direct analysis of sedimentation equilibrium distributions reflecting equilibrium complex formation between two dissimilar macromolecular solutes.

## THEORY

To characterize the interaction between an acceptor, A, possessing several sites for a macromolecular ligand, S, a mixture with defined molar concentrations of the two constituents,  $(\bar{C}_A)_0$  and  $(\bar{C}_S)_0$ , is subjected to ultracentrifugation at angular velocity  $\omega$  and temperature *T*. After attainment of chemical as well as sedimentation equilibrium, the distributions of the various species are given by the expression (*i* = A, S, AS, AS<sub>2</sub>, etc.)

$$z_i(r) = z_i(r_F) \exp[M_i \phi_i(r^2 - r_F^2)] \quad (1a)$$

$$\phi_i = (1 - \bar{v}_i \rho) \omega^2 / (2RT) \quad (1b)$$

which relates the molar thermodynamic activity, defined at constant chemical potential of solvent, of each species at any radial distance *r*,  $z_i(r)$ , to its value at some fixed radial distance,  $z_i(r_F)$ . *M<sub>i</sub>* and *v<sub>i</sub>* are the molecular weight and partial specific volume respectively of species *i*, and  $\rho$  is

<sup>†</sup> This investigation was supported by the Australian Research Council (D.J.W.). Financial contributions by the National Health and Medical Research Council of Australia and the Ramaciotti Foundation toward purchase of the Beckman XL-A analytical ultracentrifuge are also gratefully acknowledged.

\* Address correspondence to this author at the Department of Biochemistry, University of Queensland, Brisbane, QLD 4072, Australia. (FAX) 61–7–3365–4699; (E-mail) winzor@biosci.uq.edu.au.

<sup>‡</sup> University of Queensland.

<sup>§</sup> Present address: Boston Biomedical Research Institute, Boston, Massachusetts 02114-2500.

<sup>||</sup> University of Auckland; on study leave at the Santa Fe Institute.

the solvent density (6, 10).  $R$  is the universal gas constant. Because the distributions of individual species are not recorded separately, the method of analysis to be applied to an experimental record must depend upon the combination of species distributions that comprise the particular experimental profile. We shall consider three possible situations and shall assume thermodynamically ideal behavior in this initial study so that molar thermodynamic activities,  $z_i(r)$ , may be replaced by molar concentrations,  $C_i(r)$ .

*Equilibrium Distributions for Both Constituents Available.* First we consider the simplest situation; namely, that in which the instrument's optical system allows access to the radial dependence of the separate concentrations of acceptor and ligand constituents,  $\bar{C}_A(r)$  and  $\bar{C}_S(r)$ —a situation that can be realized when the quantitative contribution of each constituent (A or S) to the experimental distribution is independent of the extent of complex formation. For the total (or constituent) concentration of ligand at any radial distance,  $r$ , we may write

$$\bar{C}_S(r) = C_S(r) + K_1 C_A(r) C_S(r) + 2K_2 C_A(r) [C_S(r)]^2 + \dots \quad (2)$$

where  $K_1$ ,  $K_2$ , etc., are stoichiometric constants for formation of species AS, AS<sub>2</sub>, etc., from acceptor and ligand. To render eq 2 more akin to eq 1 we introduce the  $\psi$  function (6), defined as

$$\psi_i(r) = \exp[M_i \phi_i (r^2 - r_F^2)] \quad (3)$$

which allows eq 2 to be written in the form

$$\bar{C}_S(r) = C_S(r_F) \psi_S(r) + K_1 C_A(r_F) C_S(r_F) \psi_A(r) \psi_S(r) + 2K_2 C_A(r_F) [C_S(r_F)]^2 \psi_A(r) \psi_S(r)^2 + \dots \quad (4)$$

The advantage of expressing eq 2 in this manner is that  $C_S(r_F)$  and  $C_A(r_F)$  are constants for each recorded analyzed distribution and therefore are amenable to evaluation as curve-fitting parameters from the dependence of  $\bar{C}_S(r)$  upon  $\psi_S(r)$  and  $\psi_A(r)$ , two functions derived from separate experiments on the individual reactants (eq 3). Indeed, because  $\psi_A(r)$  and  $\psi_S(r)$  are interdependent functions related by the expression

$$\psi_A(r) = [\psi_S(r)]^p \quad p = (\phi_A M_A) / (\phi_S M_S) \quad (5)$$

the total ligand concentration may be written in terms of the single variable  $\psi_S(r)$  as

$$\bar{C}_S(r) = C_S(r_F) \psi_S(r) + K_1 C_A(r_F) C_S(r_F) [\psi_S(r)]^{(p+1)} + 2K_2 C_A(r_F) [C_S(r_F)]^2 [\psi_S(r)]^{(p+2)} + \dots \quad (6)$$

Because radial distance and hence  $\psi_S(r)$  are independent variables, nonlinear regression analysis of the dependence of total ligand concentration upon  $\psi_S(r)$  in terms of eq 6 therefore has the potential, in principle, to provide magnitudes of  $C_A(r_F)$ ,  $C_S(r_F)$ ,  $K_1$ ,  $K_2$ , etc., as curve-fitting coefficients. However, commencing analysis under the null hypothesis of 1:1 stoichiometry, it is convenient to divide eq 6 by  $\psi_S(r)$  to obtain

$$\bar{C}_S(r)/\psi_S(r) = C_S(r_F) + K_1 C_A(r_F) C_S(r_F) [\psi_S(r)]^p + 2K_2 C_A(r_F) [C_S(r_F)]^2 [\psi_S(r)]^{(p+1)} + \dots \quad (7)$$

An initial estimate of the concentration of free ligand at the reference radial position may thus be obtained as the ordinate intercept of a plot of  $\bar{C}_S(r)/\psi_S(r)$  versus  $[\psi_S(r)]^p$ , this analysis being independent of any model of the reaction stoichiometry. Thus, although nonlinear least-squares curve-fitting to eq 6 should also yield  $C_S(r_F)$  as the linear coefficient, the corresponding analysis in terms of eq 7 is considered to provide readier qualitative information on the likely stoichiometry of the interaction.

Determination of the value of  $C_S(r_F)$  allows the calculation of free ligand concentration,  $C_S(r) = C_S(r_F) \psi_S(r)$ , throughout the sedimentation equilibrium distribution. Furthermore, because the distribution for total acceptor,  $\bar{C}_A(r)$ , is also available, the binding function,  $\nu(r)$ , may then be calculated (11) as

$$\nu(r) = [\bar{C}_S(r) - C_S(r)] / \bar{C}_A(r) \quad (8)$$

Provided that  $C_S(r)$  varies sufficiently across the sedimentation equilibrium distribution (or, indeed, a series of equilibrium distributions), a binding curve may be generated by plotting  $\nu(r)$  as a function of  $C_S(r)$ . Binding constants ( $K_1$ ,  $K_2$ , etc.) may then be obtained by nonlinear regression analysis in terms of the expression (11)

$$\nu(r) = K_1 C_S(r) / [1 + K_1 C_S(r)] + K_2 C_S(r) / [1 + K_2 C_S(r)] + \dots \quad (9)$$

Introduction of the second source of experimental information,  $\bar{C}_A(r)$  versus  $r$ , into the dependent variable,  $\nu(r)$  in this manner has the advantage that it allows presentation of the sedimentation equilibrium results for the ovalbumin–cytochrome *c* interaction as a binding curve—the traditional format for ligand-binding studies.

*Equilibrium Distribution for Only One Constituent Available.* We now consider the situation in which one constituent (A or S) is not detected by the optical system used to record the sedimentation equilibrium distribution. For example, if A were a polysaccharide and S a protein, the distribution recorded by the Beckman XL-A ultracentrifuge would be the absorbance at (say) 280 nm, which would only reflect the ligand constituent (free S and the ligand contributions from AS, AS<sub>2</sub>, etc.). Clearly, the experimenter is in a less commanding position than in the previous case with access to the radial dependence of both constituent concentrations. However, for a reaction governed by 1:1 stoichiometry there is still scope for quantitative characterization provided that an experimental profile has been recorded soon after attainment of rotor speed—a routine practice for the purpose of verifying the absence of cell leakage during sedimentation equilibrium experiments.

The fact that the sedimentation equilibrium pattern records the distribution of one constituent means that  $C_S(r_F)$  may be evaluated by the application of eqs 3 and 7 if S is the constituent being monitored. Alternatively, nonlinear regression analysis in terms of eq 6 could, in principle, be applied to obtain  $K_1$ ,  $C_S(r_F)$ , and  $C_A(r_F)$ ; but again, we favor the use of eq 7. Because the approach is the same for the equilibrium

distribution in terms of either reactant, we consider only the case in which ligand is the constituent detected.

Knowledge of the concentration of free ligand at the reference radial position,  $C_S(r_F)$ , again allows access to  $\bar{C}_S(r)$ , and hence the concentration of complexed ligand,  $[C_S(r) - C_S(r_F)]$ , throughout the distribution; but the application of eq 8 is precluded by the absence of the distribution of total acceptor constituent. Indeed, the only position at which the total concentration of acceptor is of known magnitude is the hinge point,  $r_H$ , where  $\bar{C}_A(r_H) = (\bar{C}_A)_0$ , the concentration loaded into the cell. Comparison of the initial and equilibrium profiles has the potential to allow the identification of  $r_H$ , a radial position at which magnitudes may thus be assigned to  $\bar{C}_A(r_H)$ ,  $C_S(r_H)$ , and  $[C_S(r_H) - C_S(r_F)]$ . Calculation of the concentration of free acceptor at the hinge point,  $C_A(r_H)$ , as the difference between  $\bar{C}_A(r_H)$  and  $[C_S(r_H) - C_S(r_F)]$  then allows the magnitude of  $C_A(r)$  to be determined throughout the distribution. Specifically,  $C_A(r) = C_A(r_H)\psi_A(r)$  where  $\psi_A(r)$  is calculated from eq 2 with  $r_H$  as the fixed radial position. The fact that the concentrations of all three species,  $C_S(r)$ ,  $C_{AS}(r) = [\bar{C}_S(r) - C_S(r)]$ , and  $C_A(r)$ , are now available throughout the sedimentation equilibrium distribution clearly allows the magnitude of the association constant,  $K_1$ , to be determined. On the basis of the law of mass action written for a 1:1 interaction in the form

$$[\bar{C}_S(r) - C_S(r)]/C_A(r) = K_1 C_S(r) \quad (10)$$

our suggested procedure is to obtain  $K_1$  from the slope of the linear dependence of  $[\bar{C}_S(r) - C_S(r)]/C_A(r)$  upon  $C_S(r)$ . Significant curvature of the suggested plot would signify nonconformity with the presumed 1:1 reaction stoichiometry and hence invalidity of that analysis.

*Equilibrium Distribution Reflecting Both Constituents.* The remaining situation to be considered is that in which the recorded distribution reflects combined contributions of acceptor and ligand constituents. Examples include Rayleigh interferograms of the equilibrium distribution and also the  $A_{280}$  profile for a protein–protein interaction (12). This is the situation considered in the initial development of a direct analysis of heterogeneous association by sedimentation equilibrium (8). We now outline the  $\psi$  adaptation (6) of that procedure based on the  $\Omega$  function.

Because the recorded parameter, e.g., total absorbance  $A_t$ , is the sum of contributions from different species, each characterized by its own absorption coefficient ( $\epsilon_i$ ), the distribution cannot be converted directly to one in concentration unless those absorption coefficients all happen to be identical. Nevertheless, as shown by Nichol et al. (8), information on the thermodynamic activity of the smallest sedimenting species (S) may still be obtained by  $\Omega$  analysis of the total absorbance distribution. In terms of the  $\psi$  analysis, the counterpart of eq 7 becomes

$$A_t(r)/\psi_S(r) = A_S(r_F) + A_A(r_F)[\psi_S(r)]^{(p-1)} + A_{AS}(r_F)[\psi_S(r)]^p + \dots \quad (11)$$

which signifies that the dependence of  $A_t(r)/\psi_S(r)$  upon  $[\psi_S(r)]^{(p-1)}$  has an ordinate intercept of  $A_S(r_F)$ . Evaluation

of  $A_S(r_F)$  by such means allows delineation of  $A_S(r) = A_S(r_F)\psi_S(r)$  and hence  $C_S(r) = A_S(r)/\epsilon_S$  throughout the distribution.

Subtraction of  $A_S(r)$  from  $A_t(r)$  yields a revised absorbance distribution,  $A_t'(r)$  versus  $r$ , in which A now becomes the smallest macromolecular species. This residual distribution may therefore be analyzed according the expression

$$A_t'(r) = A_A(r_F)\psi_A(r) + A_{AS}(r_F)\psi_{AS}(r) + \dots \quad (12)$$

or, on division by  $\psi_A(r)$  and retention of  $\psi_S(r)$  as the independent variable

$$A_t'(r)/[\psi_S(r)]^p = A_A(r_F) + A_{AS}(r_F)[\psi_S(r)] + \dots \quad (13)$$

An estimate of  $A_A(r_F)$  may thus be determined as the ordinate intercept of a plot of  $A_t'(r)/[\psi_S(r)]^p$  versus  $[\psi_S(r)]$ ; and hence  $A_A(r)$  as  $A_A(r_F)[\psi_S(r)]^p$  throughout the distribution. Division of these values by the absorption coefficient for A,  $\epsilon_A$ , yields the corresponding values of  $C_A(r)$ .

Having obtained the molar concentrations of free acceptor and free ligand throughout the distribution, it remains to rationalize the residual absorbance,  $\Delta A_t(r) = A_t(r) - A_A(r) - A_S(r)$ , in terms of the relationship

$$\Delta A_t(r) = K_1 \epsilon_{AS} C_A(r) C_S(r) + K_2 \epsilon_{AS_2} C_A(r) [C_S(r)]^2 + \dots \quad (14)$$

where it is assumed that  $\epsilon_{AS} = (\epsilon_A + \epsilon_S)/2$  and  $\epsilon_{AS_2} = (\epsilon_A + 2\epsilon_S)/3$ , etc. By analogy with the procedure described above, eq 14 is written as

$$\Delta A_t(r)/C_A(r) = K_1 \epsilon_{AS} C_S(r) + K_2 \epsilon_{AS_2} [C_S(r)]^2 + \dots \quad (15)$$

which allows the association constants to be obtained from the best-fit description of  $\Delta A_t(r)/C_A(r)$  as a polynomial in  $C_S(r)$ .

*Direct Analysis of the Total Ligand Distribution for 1:1 Interactions.* As mentioned in relation to eq 4, an alternative approach to the characterization of heterogeneous associations is to analyze the dependence of  $\bar{C}_S(r)$  upon  $\psi_S(r)$  in terms of eq 6. Although this procedure was considered to place unreasonable demands on the precision and accuracy of experimental distributions in situations where the stoichiometry could well exceed unity, it does offer potential for the characterization of 1:1 complex formation—particularly in instances where equilibrium distributions are available experimentally for both constituents.

For a 1:1 interaction, the expression describing total ligand concentration (eq 6 with  $K_2 = 0$ ) still contains three parameters,  $C_S(r_F)$ ,  $C_A(r_F)$ , and  $K$ , whose magnitudes would need to be obtained by regression analysis with  $\psi_S(r)$  as the independent variable. However, this number can be decreased to two by eliminating  $C_A(r_F)$  on the grounds that

$$C_A(r_F) = \bar{C}_A(r_F) - \bar{C}_S(r_F) + C_S(r_F) \quad (16)$$

for a system with AS as the only complex. With this substitution the simplified version of eq 6 (with  $K_2 = 0$  and  $K \equiv K_1$ ) becomes



$$\bar{C}_S(r) = C_S(r_F)\psi_S(r) + K\{\bar{C}_A(r_F) - \bar{C}_S(r_F) + C_S(r_F)\}\bar{C}_S(r_F)[\psi_S(r)]^{(p+1)} \quad (17)$$

whereupon the two parameters to be obtained by curve-fitting are  $C_S(r_F)$  and the product  $K\{\bar{C}_A(r_F) - \bar{C}_S(r_F) + C_S(r_F)\}$ , in which the difference between the two constituent concentrations is of known magnitude. Because the only information that is used from the second distribution is the constituent concentration at  $r_F$ , selection of the hinge point ( $r_H$ ) as the fixed radial distance would allow this method to be applied also to sedimentation equilibrium experiments for which the distribution of only one constituent (A or S) is available.

A limitation inherent in such use of eq 17 is, of course, the difficulty of accommodating data from different sedimentation equilibrium experiments because the value of  $C_S(r_F)$  refers specifically to the mixture with the composition  $[\bar{C}_A(r_F), \bar{C}_S(r_F)]$  prevailing at the reference radial position in a particular experiment. However, results from different sedimentation equilibrium experiments may be accommodated in a global analysis by rewriting the truncated form of eq 6 as

$$\bar{C}_S(r) = \bar{C}_S(r_F)\psi_S(r) + C_{AS}(r_F)[\psi_S(r)]^{(p+1)} \quad (18)$$

where  $[\psi_S(r)]^{(p+1)} \equiv \psi_{AS}(r)$ .  $C_S(r_F)$  and  $C_{AS}(r_F)$  may thus be obtained as the two coefficients evaluated by regression analysis of the dependence of  $\bar{C}_S(r)$  upon  $\psi_S(r)$ . Global analysis of such parameters from a series of sedimentation equilibrium distributions is then effected by their combination with the appropriate value of  $\bar{C}_A(r_F)$  for each distribution in the expression

$$C_{AS}(r_F)/[\bar{C}_A(r_F) - C_{AS}(r_F)] = KC_S(r_F) \quad (19)$$

to obtain  $K$  as the slope of the dependence of  $C_{AS}(r_F)/[\bar{C}_A(r_F) - C_{AS}(r_F)]$  upon  $C_S(r_F)$ .

## EXPERIMENTAL PROCEDURES

Bovine heart cytochrome *c* (type 5) and ovalbumin (grade V) were preparations obtained from Sigma Chemical Co., St. Louis, MO. These protein preparations were dissolved in 0.05 M 2-(*N*-morpholino)ethanesulfonic acid/NaOH, pH 6.3, *I* 0.03, after which the separate solutions were dialyzed against more of the same buffer to attain dialysis equilibrium. On the grounds that sedimentation equilibrium experiments on the solution of ovalbumin failed to yield distributions commensurate with its molecular weight of 45 000, a concentrated solution (1 mL, 10 mg/mL) was subjected to zonal gel chromatography at 0.5 mL/min on a column of Sephadex G-200 (1.0 × 30 cm) preequilibrated with the same buffer. This exclusion chromatography step not only removed the contaminating material but also provided a purified solution in dialysis equilibrium with the buffer to be used in the subsequent sedimentation equilibrium studies. Concentrations of protein solutions were based on molar absorption coefficients of 29 700 and 23 200 M<sup>-1</sup> cm<sup>-1</sup> at 280 nm for ovalbumin (13) and cytochrome *c* (14), respectively.

Solutions of the separate protein reactants and mixtures thereof in 12-mm double-sector cells were subjected to centrifugation at 20 °C and either 15 000 or 20 000 rpm in

Table 1: Range of Constituent Concentrations Covered in Sedimentation Equilibrium Experiments on Mixtures of Ovalbumin (A) and Cytochrome *c* (S)

expt no.	speed (rpm)	$\bar{C}_A(r)$ (μM)	$\bar{C}_S(r)$ (μM)
1 <sup>a</sup>	15 000	1.3–20.3	5.2–20.6
2	15 000	1.3–17.6	5.3–16.7
3	15 000	0.6–23.2	5.0–11.0
4	15 000	2.0–6.4	9.8–20.1
5	15 000	0.1–7.8	9.2–20.9
6	15 000	2.6–20.5	1.3–4.9
7	15 000	3.4–14.8	1.4–3.9
8	15 000	2.4–24.0	1.4–5.7
9	15 000	0.1–10.4	3.2–10.1
10	15 000	0.2–13.0	3.3–11.8
11	20 000	0.5–25.0	0.3–2.7
12	20 000	0.1–18.5	0.3–2.3
13	20 000	0.6–15.8	0.4–1.9
14	20 000	0.2–21.8	0.1–1.4
15	20 000	1.7–28.5	0.1–1.1

<sup>a</sup> Experiment reported in Figure 3.

a Beckman XL-A analytical ultracentrifuge for approximately 24 h, and the resulting equilibrium distributions were recorded spectrophotometrically at 280 and/or 410 nm: comparison of distributions obtained during the progress of runs on these 2.5–3.2 mm liquid columns had established their essential superimposition after about 16 h of centrifugation. The operational extinction coefficient of cytochrome *c* at the higher wavelength (106 000 M<sup>-1</sup> cm<sup>-1</sup>) was based on that at 280 nm and the ratio of absorbances at the two wavelengths for a solution of cytochrome *c*. Partial specific volumes of the two proteins were taken as 0.748 mL/g for ovalbumin (15) and 0.728 mL/g for cytochrome *c* (16). The density of the buffer (diffusate) was determined as 0.9999 g/mL at 20 °C by standard procedures in an Anton Paar density meter.

The sedimentation equilibrium distribution recorded in terms of  $A_{410}(r)$  for mixtures of cytochrome *c* (S) and ovalbumin (A) reflects solely the radial dependence of the concentration of cytochrome *c* constituent,  $\bar{C}_S(r)$ , obtained by dividing the values of  $A_{410}(r)$  by the molar absorption coefficient of cytochrome *c* at this wavelength; the corresponding absorbances for the S constituent at 280 nm were also calculated from the molar absorption coefficient of cytochrome *c* at that wavelength. After first checking the validity of assuming absorbance additivity in mixtures of the two reactants, values of  $A_{280}(r)$  for the ovalbumin, and hence of  $\bar{C}_A(r)$ , were obtained by subtracting the S-constituent absorbance from the total absorbance at this wavelength. The consequent availability of separate sedimentation equilibrium distributions for the ovalbumin and cytochrome *c* constituents allowed maximal advantage to be taken of the quantitative expressions developed in the previous section for the characterization of equilibria involving dissimilar macromolecular reactants. Table 1 summarizes the lower and upper limits of the constituent concentrations,  $\bar{C}_S(r)$  and  $\bar{C}_A(r)$ , in the 15 sedimentation equilibrium distributions used to characterize the interaction between ovalbumin and cytochrome *c*.

## RESULTS

Selection of ovalbumin and cytochrome *c* as the two reactants of the model system was clearly based on the existence of a convenient chromophore on the latter to allow

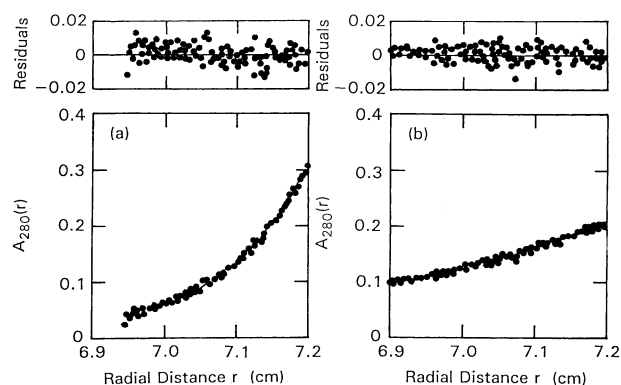


FIGURE 1: Sedimentation equilibrium distributions obtained at 15 000 rpm and 20 °C for (a) ovalbumin and (b) cytochrome *c*, together with the best-fit descriptions in terms of reduced molecular weights of  $0.583 (\pm 0.019)$  and  $0.184 (\pm 0.008)$ , respectively.

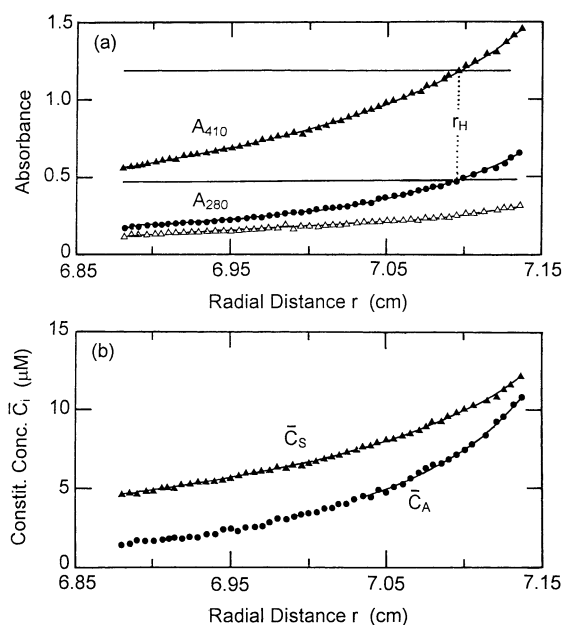


FIGURE 2: Sedimentation equilibrium distributions obtained at 15 000 rpm and 20 °C for an interacting mixture comprising 7.16  $\mu\text{M}$  ovalbumin (A) and 9.77  $\mu\text{M}$  cytochrome *c* (S). (a) Distributions in terms of absorbances at 410 ( $\blacktriangle$ ) and 280 ( $\bullet$ ) nm, together with the estimated contribution ( $\triangle$ ) of the cytochrome *c* constituent at 280 nm. (b) Concentration distributions for the separate constituents deduced from panel a.

the delineation of its constituent concentration,  $\bar{C}_S(r)$ , throughout the sedimentation equilibrium distribution. The fact that ovalbumin is an acidic protein (*pI* 4.6) whereas cytochrome *c* is basic (*pI* 10.4) guarantees some form of electrostatic interaction between the two reactants at low ionic strength and near-neutral pH. On the basis of the limited charge data available for cytochrome *c* (17) and ovalbumin (18), the two reactants should bear net charges of approximately equal magnitude but opposite sign in the range pH 6.0–6.5. The fact that the AS complex is thus likely to bear essentially zero net charge should render negligible the formation of complexes with greater than 1:1 stoichiometry under the conditions of study (pH 6.3, *I* 0.03).

Distributions for ovalbumin and cytochrome *c* in sedimentation equilibrium experiments conducted at 15 000 rpm are presented in Figure 1, panels a and b, respectively. Nonlinear regression analysis of these distributions according to eq 1 with  $A_{280}(r)$  substituted for  $z_i(r)$  yielded a reduced

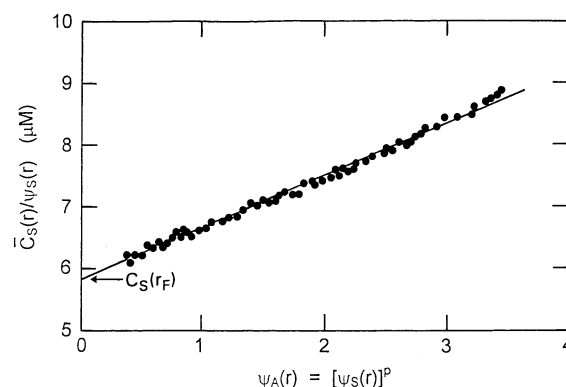


FIGURE 3: Analysis of the distribution for cytochrome *c* constituent (Figure 2b) in accordance with eq 7 to evaluate  $C_S(r_F)$ , the concentration of free cytochrome *c* at the selected reference radial position ( $r_F = 7.000$  cm).

molecular weight,  $M_i(1 - \bar{v}_i\rho)\omega^2/(2RT)$ , that translated into respective molecular weights of 45 700 ( $\pm 1500$ ) and 13 400 ( $\pm 600$ ) for ovalbumin and cytochrome *c*, respectively—values commensurate with those deduced from sequence data.

**Analyses Reliant upon Availability of Both Constituent Concentration Distributions.** To commence this illustration of various analytical procedures developed in the Theory section, we consider the situation in which separate distributions are available for the acceptor (ovalbumin) and ligand (cytochrome *c*) constituents. Figure 2a summarizes the sedimentation equilibrium distributions recorded at 410 nm ( $\blacktriangle$ ) and 280 nm ( $\bullet$ ) for a mixture of ovalbumin (7.16  $\mu\text{M}$ ) and cytochrome *c* (9.77  $\mu\text{M}$ ) subjected to centrifugation at 15 000 rpm and 20 °C. Because the distribution at the higher wavelength reflects only the cytochrome *c* constituent, the corresponding distribution in terms of total cytochrome *c* ( $\bar{C}_S$ ) was obtained by incorporating the absorption coefficient at that wavelength ( $\blacktriangle$ , Figure 2b). On the basis of the relative magnitudes of the absorption coefficients of cytochrome *c* at 280 and 410 nm, the contribution of the S constituent to the distribution recorded at 280 nm is also shown ( $\triangle$ ) in Figure 2a, whereupon division of the residual absorbance at 280 nm by the absorption coefficient of ovalbumin yielded the sedimentation equilibrium distribution for ovalbumin constituent ( $\bar{C}_A$ ) shown ( $\bullet$ ) in Figure 2b: the magnitude of each  $\bar{C}_A(r)$  does, of course, reflect any experimental error in  $\bar{C}_S(r)$ .

Analysis of the distribution for cytochrome *c* in terms of eq 7 with  $r_F = 7.000$  cm in a solution column with radial limits of 6.880 and 7.200 cm is summarized in Figure 3, where the distributions have been terminated at  $r = 7.150$  cm because of the high absorbance at 410 nm. Several points are noted. First, the essentially linear form of the dependence of  $\bar{C}_S(r)/\psi_S(r)$  upon  $\psi_A(r)$  indicates the dominance of 1:1 complex formation between cytochrome *c* and ovalbumin under the present conditions. Second, the virtual linearity of Figure 3 also renders fairly accurate the extrapolation to obtain  $C_S(r_F)$  as the ordinate intercept: a value ( $\pm 2$  SD) of  $5.83 (\pm 0.02)$   $\mu\text{M}$  is obtained by polynomial curve-fitting, irrespective of the term at which the polynomial is truncated. Third, consideration of the linear form of Figure 3 to signify the formation of a single 1:1 complex also allows identification of  $C_{AS}(r_F)$  with the slope. Combination of that estimate of  $0.83 (\pm 0.02)$   $\mu\text{M}$  for  $C_{AS}(r_F)$  with the above value of

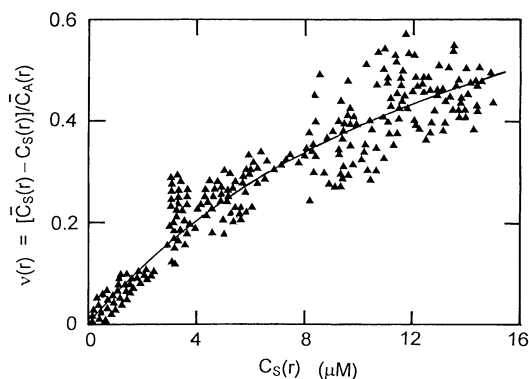


FIGURE 4: Characterization of the interaction of cytochrome *c* with ovalbumin by means of the binding curve obtained by the application of eq 8 to sedimentation equilibrium distributions for the separate constituents, i.e.,  $\bar{C}_S(r)$  and  $\bar{C}_A(r)$  as a function of radial distance (Figure 2b and corresponding data from 14 other experiments). The solid line denotes the best-fit description obtained by nonlinear regression analysis in terms of the rectangular hyperbolic relationship for 1:1 complex formation (eq 9 with  $K_2 = 0$ ).

$C_S(r_F)$  and a  $C_A(r_F)$  of 3.32  $\mu\text{M}$  yields an association constant ( $K$ ) of 57 000 ( $\pm 3000$ )  $\text{M}^{-1}$  for 1:1 interaction between ovalbumin and cytochrome *c*. However, at this stage we prefer to maintain model independence of the analysis and hence proceed solely on the basis that Figure 3 has sufficed to define  $C_S(r_F)$ .

To complete the analysis, eq 1 was then used to evaluate the sedimentation equilibrium distribution of free cytochrome *c*, which was then combined with the distributions in terms of  $\bar{C}_S(r)$  and  $\bar{C}_A(r)$  (Figure 2b) to evaluate the binding function (eq 8) as a function of  $C_S(r)$ . Results from that sedimentation equilibrium experiment as well as 14 others are presented as a binding curve in Figure 4, where, for the sake of clarity, the plot contains every tenth experimental point. Nonlinear curve-fitting of the entire data set to the rectangular hyperbolic relationship for 1:1 complex formation (eq 9 with  $K_2 = 0$ ) yields an association constant of 63 000 ( $\pm 2000$ )  $\text{M}^{-1}$ , where twice the standard deviation is used to express the uncertainty. No improvement in fit is accomplished by regression analysis in terms of the untruncated version of eq 9; and fitting to the general rectangular hyperbolic relationship, viz.,  $v(r) = nKC_S(r)/[1 + KC_S(r)]$ , leads to an estimate of 0.9 ( $\pm 0.1$ ) for  $n$ , the number of sites for cytochrome *c* on ovalbumin. We therefore conclude that the electrostatic interaction between ovalbumin and cytochrome *c* under the present conditions (pH 6.3,  $I$  0.03) is confined to 1:1 stoichiometry and governed by an association constant of approximately 63 000  $\text{M}^{-1}$ .

The fact that the interaction being characterized is described adequately by 1:1 stoichiometry opens up the possibility that a reasonable characterization might also arise from nonlinear regression analysis of the distributions in terms of eq 17 with  $p = 3.2$  (the experimentally determined value) to obtain  $C_S(r_F)$  and  $C_{AS}(r_F)$  as the two curve-fitting parameters for each distribution. Global analysis of those results from the 15 experiments in accordance with eq 19 is summarized in Figure 5, from which an association constant of 60 000 ( $\pm 12 000$ )  $\text{M}^{-1}$  is obtained. In that regard the greater uncertainty in this estimate compared with that from Figure 4 simply reflects the smaller number of observations as the result of summarizing each sedimentation equilibrium

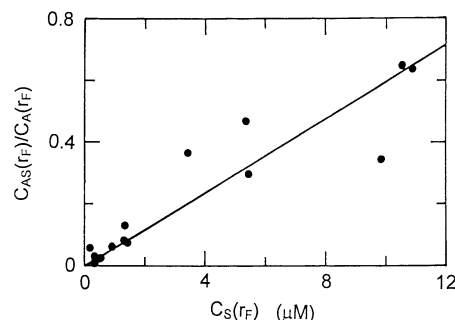


FIGURE 5: Alternative, model-dependent characterization of the interaction between cytochrome *c* and ovalbumin by sedimentation equilibrium, the results for the ligand constituent,  $\bar{C}_S(r)$ , being analyzed in accordance with eqs 18 and 19, which only apply to ideal interactions governed by 1:1 stoichiometry.

distribution in terms of a single point, that is,  $[C_{AS}(r_F)/\{\bar{C}_A(r_F) - C_{AS}(r_F)\}, C_S(r_F)]$ .

**Characterization from the Distribution for Only One Constituent.** By restricting consideration to the sedimentation equilibrium distribution at 410 nm, we are able to illustrate the feasibility of characterizing (for example) a polysaccharide–protein interaction solely from the distribution of the protein distribution recorded by the absorption optical system of an XL-A ultracentrifuge. Analysis of the one distribution available (cytochrome *c* constituent in this case) follows the procedure already illustrated in Figure 3, except that the reference radial position ( $r_F$ ) must be chosen to coincide with the hinge point. From the intersection point of the initial (horizontal line) and equilibrium distributions at 410 nm (Figure 2a),  $r_H = 7.095$  cm, a value confirmed in this particular example by the corresponding intersection point for the two distributions recorded at 280 nm. Analysis of the ligand constituent distribution in terms of eq 7 with  $r_F = r_H = 7.095$  cm (Figure 6a) yields a  $C_S(r_H)$  of 7.16 ( $\pm 0.04$ )  $\mu\text{M}$  in a mixture with  $\bar{C}_S(r_H) = 9.77$   $\mu\text{M}$  and  $\bar{C}_A(r_H) = 7.16$   $\mu\text{M}$  (the composition of the mixture placed in the centrifuge cell). Evaluation of  $C_S(r)$  as  $\psi_S(r)C_S(r_F)$  and  $C_A(r)$  as  $\psi_A(r)C_A(r_F)$  with  $C_A(r_F) = \bar{C}_A(r_F) - C_S(r_F) + C_S(r_F)$  throughout the distribution allows  $K$  to be determined from the plot of results according to eq 10 (Figure 6b): the association constant of 63 000 ( $\pm 4000$ )  $\text{M}^{-1}$  agrees well with the value of 57 000 ( $\pm 3000$ )  $\text{M}^{-1}$  deduced from Figure 3, which also refers to this particular experiment.

**Analysis of an Equilibrium Distribution Reflecting Both Constituents.** This most unfavorable situation entails characterization of the ovalbumin–cytochrome *c* interaction solely from the sedimentation equilibrium distribution at 280 nm. The application of eq 11 to obtain the absorbance contribution of smallest solute species (cytochrome *c*, S), is presented (●) in Figure 7, for which  $r_F = 7.095$  cm (the hinge point as in Figure 6a). In contrast with its predecessors (Figures 3 and 6a), this  $\psi$  plot is curvilinear—an indication that the distribution reflects the contribution of more than one species (A as well as AS) in addition to that of free ligand. Linear regression analysis of data in the range 0.3  $< [\psi_S(r)]^{p-1} < 0.7$  yields an estimate of 0.203 ( $\pm 0.007$ ) for  $A_S(r_F)$ , which is then used to evaluate  $A_S(r)$  for subtraction from the total absorbance,  $A_t(r)$ , to obtain a revised distribution,  $A_t'(r)$  versus  $r$ , in which acceptor (ovalbumin) now becomes the smallest species. The corresponding analysis



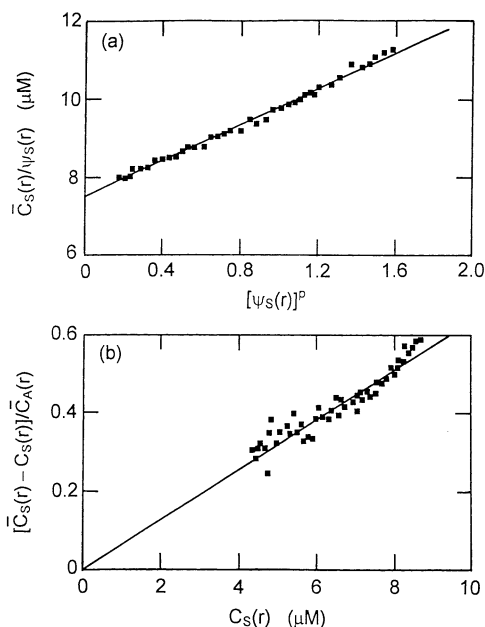


FIGURE 6: Characterization of the ovalbumin–cytochrome *c* interaction by analysis of the sedimentation equilibrium distribution recorded at 410 nm. (a)  $\psi$  plot for determination of  $C_S(r_H)$  via eq 7 with the hinge point ( $r_H$ ) chosen as the fixed radial position ( $r_F$ ). (b) Consequent plot of the results in accordance with eq 10 for evaluation of the equilibrium constant.

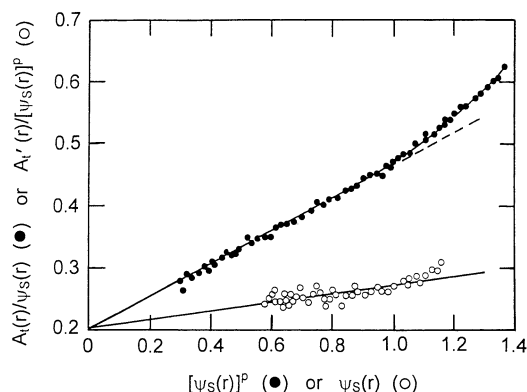


FIGURE 7: Characterization of the ovalbumin–cytochrome *c* interaction by analysis of the sedimentation equilibrium distribution recorded at 280 nm: ●, analysis of the distribution in accordance with eq 11 to obtain the absorbance contribution,  $A_S(r_F)$ , of free cytochrome *c*; ○, corresponding analysis of the residual absorbance distribution in accordance with eq 13 to obtain  $A_A(r_F)$  and  $A_{AS}(r_F)$  from the ordinate intercept and slope, respectively. The broken line is a continuation of the limiting tangent used for the estimation of  $A_S(r_F)$ .

of that distribution in terms of eq 12 is also shown (○) in Figure 7. On the grounds that the revised distribution reflects only A and AS, the results have been subjected to linear regression analysis to obtain values of  $0.202 (\pm 0.012)$  for  $A_A(r_F)$  and  $0.070 (\pm 0.015)$  for  $A_{AS}(r_F)$  from the ordinate intercept and slope, respectively. Substitution of the three species concentrations so obtained [ $C_S(r_F) = 8.8 (\pm 0.3) \mu\text{M}$ ,  $C_A(r_F) = 6.8 (\pm 0.4) \mu\text{M}$ , and  $C_{AS}(r_F) = 2.6 (\pm 0.6) \mu\text{M}$ ] in the expression for the association equilibrium constant yields  $K = 43\,000 (\pm 13,000) \text{ M}^{-1}$ .

The source of the discrepancy between this estimate and the earlier values of the equilibrium constant is readily traced. Analysis of the total absorbance distribution at 280 nm has led to an estimate of  $C_S(r_F)$  that is 18% higher than the value

deduced from the corresponding  $\psi$  plot of the  $A_{410}$  distribution (Figure 6a). Calculated values for the  $A_S(r)$  distribution also reflect this discrepancy, which is then incorporated as a systematic error into the revised distribution,  $A'_t(r)$  versus  $r$ , upon which the evaluations of  $C_A(r_F)$  and  $C_{AS}(r_F)$  are based. Such incorporation of systematic error into the analysis is clearly undesirable and should be avoided whenever possible. However, as demonstrated in a recent sedimentation equilibrium study of the interaction between electron transferring flavoprotein and trimethylamine dehydrogenase (12), circumstances do arise in which all other options are precluded. In that light it is comforting to note that, despite its shortcomings, this least-desirable procedure has still provided a reasonable estimate of the equilibrium constant.

## DISCUSSION

As noted in the introduction, the aim of this investigation has been to develop direct, rather than iterative curve-fitting, approaches to the characterization of interactions between dissimilar macromolecular reactants by sedimentation equilibrium, thereby resuming an endeavor (8) that had languished for two decades. To that end, improved procedures have been suggested for various situations that are likely to be encountered experimentally. From the viewpoints of accuracy and precision of the resulting estimates, the preferred situation entails analysis of separate equilibrium distributions for the two constituents: the experiment then generates the maximum amount of data on which to base the characterization. For the benefit of those engaged in studies of protein–polysaccharide interactions by ultracentrifugation in the XL-A, a comparable analysis can be used in instances where the equilibrium distribution of only one constituent is available by taking advantage of the fact that the total concentration of nonrecorded reactant is of defined magnitude at the hinge point. The least desirable situation entails sedimentation equilibrium of an interacting system for which the only distribution available is in terms of combined contributions from both constituents.

The optimal procedure used to characterize the interaction between cytochrome *c* and ovalbumin (Figures 2–4) differs markedly from its recent counterparts for analysis of heterogeneous association (1, 2) in that the emphasis is on the extraction of interaction parameters from the experimental distributions rather than on their evaluation by iterative simulation of distributions to seek solutions that match the experimental records. Establishment of the feasibility of employing a simple and direct analysis of the  $\bar{C}_S(r)$  distribution, and hence corresponding analysis of the  $\bar{C}_A(r)$  distribution if required, is an important outcome because such procedures are prerequisites for extending studies of heterogeneous associations to include the consequences of thermodynamic nonideality in complex formation between two dissimilar macromolecular reactants. For the thermodynamically nonideal case the analysis must be changed slightly from that used above, because the above evaluations of  $K$  have relied upon identification of thermodynamic activities,  $z_i(r)$ , with molar concentrations,  $C_i(r)$ . However, the way now seems clear for adaptation of the statistical–mechanical approach used previously (6) for the characterization of thermodynamically nonideal solute self-association.

## REFERENCES

1. Laue, T. M., Senear, D. F., Eaton, S., and Ross, A. J. B. (1993) *Biochemistry* 32, 2469–2472.
2. Kim, T., Tsukiyama, T., Lewis, M. S., and Wu, C. (1994) *Protein Sci.* 3, 1040–1051.
3. Lewis, M. S., Shrager, R. I., and Kim, S. J. (1994) in *Modern Analytical Ultracentrifugation: Acquisition and Interpretation of Data for Biological and Synthetic Polymer Systems* (Schuster, T. M., and Laue, T. M., Eds.) pp 94–115, Birkhäuser, Boston, MA.
4. Bailey, M. F., Davidson, B. E., Minton, A. P., Sawyer, W. H., and Howlett, G. J. (1996) *J. Mol. Biol.* 263, 671–684.
5. Johnson, M. L., Correia, J. J., Yphantis, D. A., and Halvorson, H. R. (1981) *Biophys. J.* 36, 575–588.
6. Wills, P. R., Jacobsen, M. P., and Winzor, D. J. (1996) *Biopolymers* 38, 119–130.
7. Milthorpe, B. K., Jeffrey, P. D., and Nichol, L. W. (1975) *Biophys. Chem.* 3, 169–176.
8. Nichol, L. W., Jeffrey, P. D., and Milthorpe, B. K. (1976) *Biophys. Chem.* 4, 259–267.
9. Jeffrey, P. D., Nichol, L. W., and Teasdale, R. D. (1979) *Biophys. Chem.* 10, 379–387.
10. Wills, P. R., Comper, W. D., and Winzor, D. J. (1993) *Arch. Biochem. Biophys.* 300, 206–212.
11. Klotz, I. M. (1947) *Arch. Biochem.* 9, 109–117.
12. Wilson, E. K., Scrutton, N. S., Cölfen, H., Harding, S. E., Jacobsen, M. P., and Winzor, D. J. (1997) *Eur. J. Biochem.* 243, 393–399.
13. Crammer, J. L., and Neuberger, A. (1943) *Biochem. J.* 37, 302–310.
14. Margoliash, E., and Frohwirt, N. (1959) *Biochem. J.* 71, 570–572.
15. Dayhoff, M. O., Perlmann, G. E., and MacInnes, D. A. (1952) *J. Am. Chem. Soc.* 74, 2515–2517.
16. Ehrenberg, A. (1957) *Acta Chem. Scand.* 11, 1257–1270.
17. Laue, T. M., Hazard, A. L., Ridgeway, T. M., and Yphantis, D. A. (1989) *Anal. Biochem.* 182, 377–382.
18. Creeth, J. M., and Winzor, D. J. (1962) *Biochem. J.* 83, 566–574.

BI972211V